A novel optimized mold release Oil-in-Water emulsion for polyurethane foams production

A. Olietti,[a] E. Pargoletti,[a,b] A. Diona,[c] G. Cappelletti[a,b,*]

[a] Università degli Studi di Milano, Dipartimento di Chimica, via Golgi 19, 20133, Milano, Italy

[b] Consorzio Interuniversitario Nazionale per la Scienza e Tecnologia dei Materiali (INSTM), via Giusti 9, 50121, Firenze, Italy

[c] Marbo Italia S.p.A., Via Torquato Tasso 27, 20010 Pogliano Milanese, Milan, Italy

E-mails: a.olietti@gmail.com; eleonora.pargoletti@unimi.it; a.diona@gruppomarbo.com

Abstract

Release agents are compounds usually sprayed on the molds surface, forming a thin film that can act as a barrier preventing the sticking. Herein, both physical and chemical optimization of a wax-based O/W emulsion for polyurethane (PU) foams is reported. E_$N_{1.8}Cet_{1.2}Ac_{2.5}$ sample (where N, Cet and Ac stand for the percentages of linear amine, cetyl alcohol and acetic acid), emulsified by the inversion point method, turned out to have the optimal composition, in terms of smaller oil droplets size (by Dynamic Light Scattering analysis and optical measurements), long-term stability (by Abbe refractometer and backscattering tests), good spreading (contact angle and surface tension measurements) and low corrosion phenomena (by potentiodynamic polarization tests, Scanning Electron Microscopy analysis). Principal Component Analysis helped to find the best correlations among all the investigated variables and to have some predictions on the role of the different raw materials in affecting the final stability of the emulsions.

Keywords

O/W emulsion; mold releasing; interfaces; emulsion stability; chemometrics; corrosion.

* Corresponding author; Università degli Studi di Milano, Dipartimento di Chimica, via Golgi 19, 20133, Milano, Italy; e-mail: giuseppe.cappelletti@unimi.it; Phone: +390250314228; Fax: +390250314228.

1. Introduction

Polyurethanes (PUs) include a wide group of polymers with different compositions and properties, which are used in a great variety of applications, *e.g.* as coatings [1], adhesives or foams [2–5]. Typically, they are produced by a polycondensation process of polyisocyanates with polyalcohols [3]. In particular, flexible PU-based foams are usually manufactured in a batch molding process, where the reactive components are premixed with catalysts, foam stabilizers, reinforcing agents and other additives, and then poured into a heated mold (up to ~80°C). The mold is then closed, allowing foam expansion, and the finished product is subsequently removed [6,7].

Therefore, to facilitate an easier and cleaner removal of the PU products, release agents are usually sprayed on the mold surface, forming a thin film that can act as a barrier preventing the PU sticking [8–11]. There are several raw materials, characterized by low surface energy, that exhibit the previous properties, such as waxes, soaps, fluorocarbon molecules and silicone oils [7,12]. These release agents can be classified into two main categories based on the type of the carrier used for their formulation, *i.e.* solvent- and water-borne agents [6,12,13]. The solvent-based carriers were the first class being developed [8]. However, due to several drawbacks related to their use (such as toxic emissions, flammability and costs), they have been widely substituted by water-based formulations [14]. Nevertheless, also aqueous systems have shown some problems concerning: *i*) the higher mold temperatures necessary to remove water due to hydrogen bondings, *ii*) water high surface tension that leads to lower releasing performances and *iii*) its high reactivity towards isocyanate that leads to the formation of unstable carbamic acid, which decomposes to the corresponding amine and carbon dioxide [13]. Moreover, the latter provokes undesired bubbles, blisters, craters and voids in the final PU product. Thus, although both carriers show some drawbacks, the waterborne agents should be favored especially due to environmental concerns.

In the last few decades, oil-in-water (O/W) emulsions have been developed to be applied also in this field [12]. Indeed, when sprayed on the hot mold, water evaporates breaking the emulsion and leaving a film with good releasing features [14]. Their general composition includes: an active release agent (*e.g.* waxes, oils, soaps, paraffins and silicones), ionic or non-ionic surfactants (for example fatty ethoxylated alcohols or amines, fatty acids or esters) [15], film forming agents (such as paraffins, aromatics or aliphatic hydrocarbons) to prevent the washing off of the release agent during the pouring procedures, the carrier

(water) and auxiliary compounds (*i.e.* catalysts such as Lewis acids or bases, foam stabilizers, viscosity modifiers, preservatives, biocides, fungicides and antioxidants) [12–14]. Hence, the nowadays challenge should be the formulation of a release agent with optimal removal features, high stability during storage, low corrosion behaviour (in the case of metallic molds) and good environmental compatibility. However, studies about this aspect are rather scarce and only patents are available so far [6,10,12,16–18].

Therefore, the present research work will be focused on the optimization of a wax-based O/W emulsion used as release agent for PU-based foams. Particularly, by analyzing data obtained varying both physical variables and chemical features of the starting emulsion, we succeeded in preparing an optimal product that showed good performances in terms of stability, low corrosion phenomena and optimal spreading behaviour (either on aluminum or polyester/epoxy molds).

2. Experimental

All the chemicals [12] were of reagent-grade purity and were used without further purification.

2.1 Wax-based O/W emulsions and mold substrates

O/W emulsions were prepared according to the general composition reported in Table 1. The wax, fully saturated homopolymers of ethylene with a high degree of linearity and crystallinity, exhibits sharp melting point, fast recrystallization, low melting viscosity, excellent heat stability and resistance to chemical attack. An aliphatic turpentine-based solvent was adopted to completely solubilize the wax, and two liquid silicones with different viscosities (*i.e.* 60 cP and 180 cP) were further added. A linear fatty amine and cetyl alcohol were utilized as surfactant/corrosion inhibitor and co-surfactant, respectively. Finally, acetic acid was used to completely solubilize the linear amine.

A 2 L glass pilot plant reactor was adopted for emulsions optimization (see Fig. S1a). The reactor has a double glass walled vessel for temperature control with a jacketed bottom Teflon drain valve; it is equipped with an external 1 L glass jacketed funnel for water heating. The stirring mechanism was provided by an anchor blade stirrer shown in Figure S1b. A silicone (50 cP) was used as the heating fluid into the mantle. Ministat 230 and CC-208B thermostats (by Huber) were utilized to record temperature gradient and cooling/stirring rates, respectively. Thus, all the materials were heated in the reactor, except for water that

was added into the external jacketed funnel (Fig. S1a). Once the solid materials became liquid, water was heated at 95°C and gradually added into the reactor. The W/O emulsion was firstly formed, then the desired O/W one was obtained through the emulsification inversion point. When all water was added, a temperature cooling rate program (down to room temperature) was set.

In order to optimize the emulsion, both physical (such as time of water addition, emulsification and cooling stirring rates) and chemical variables were investigated. Particularly as concerns the latter, the amine, alcohol and acetic acid percentages were varied (see Table 1) and three different water samples were adopted: softened, osmotized and Milli-Q one, with diverse conductivity values (*i.e.* 250, 15 and 2 μS cm^{-1}, respectively).

All samples were labeled as $E\_N_xCet_yAc_z$, where x, y and z stands for the percentages of the amine (N), cetyl alcohol (Cet) and acetic acid (Ac), respectively.

Three different types of mold materials were adopted, *i.e.* aluminum, fiberglass-coated polyester and polymer-coated epoxy resin. Both organic substrates were cleaned by ultrasounds in Milli-Q water for 15 minutes and then let them dry in air. Only for aluminum material, a cleaning treatment in 2-propanol or 5% hot oxalic acid was performed to remove all the impurities traces.

2.2 Samples characterizations

All the prepared emulsions were finely characterized by means of different physico-chemical techniques.

Emulsions stability was studied by Dynamic Light Scattering (DLS) analyses and by evaluating the height of phase separation after a heating treatment. For the former technique, analyses were carried out with diluted 4 g L^{-1} emulsion samples using a Malvern Zetasizer NANO ZS (at 25°C). The dilution did not affect the results, as already reported in the literature [19]. Measurements were performed on two different emulsions aliquots, for 30 scans each. On the contrary, the height of phase separation was evaluated by heating emulsions in closed vials at 60°C for 6 h [20]. We reported the results in terms of destabilization degree, *i.e.* the ratio between the creaming volume and the total volume of the sample. Furthermore, the samples stability was monitored by measuring the light backscattering using a Turbiscan MA2000 instrument. The emulsions were placed in a 65 mm cylindrical glass cell and the backscattering of light was

111 measured as a function of both time and cell height. A scan was recorded every 2 h, for a total of 92 h, at
112 room temperature [21,22]. Changes in the height of the creamed/settled oil with time were obtained from the
113 backscattering profiles.
114 70% by volume water-diluted emulsions were analyzed by using LEICA DMRB fluorescence
115 microscope to observe either droplets dimensions or their dispersity.
116 To check both the good emulsification and the real content of the oil phase in water, a commercial
117 analogic Abbe refractometer was also used [23]. These measurements were achieved placing the correct
118 amount of liquid sample over the refractive prism, then the sample was sandwiched into a thin layer closing
119 the illuminating prism.
120
121 *2.3 Data processing and analysis*
122 The Principal Component Analysis (PCA) was used to find connections among the different
123 investigated parameters (both physical and chemical ones) and the several emulsions formulated, either to
124 corroborate the observations made by the physico-chemical analyses or to identify/predict the most stable
125 samples. The model was developed taking into account 33 samples (*i.e.* scores) and 12 parameters (*i.e.*
126 loadings) to construct a training set (Table 2). After mean centering and autoscaling procedures, the PCA
127 model was then calculated considering five Principal Components (PCs) for a total of 85% of explained
128 variance. The loading plot (with the investigated variables) reports on x and y axes the principal components
129 (PC2 *vs* PC1, Fig. 1a and PC3 *vs* PC1, Fig. 1b), respectively. All the data have been treated by using R-based
130 Chemometrics software (by the Chemometric Group of the Italian Chemical Society).
131
132 *2.4 Interaction O/W emulsions – substrates analyses*
133 To study the interactions between emulsions and substrates, emulsions surface tension (γ_{lv}) analyses
134 were performed using digital tensiometer Gibertini following the Du-Noüy Method [23]. The liquid-solid
135 surface tension (γ_{ls}) was calculated by using the Young equation:
136 (1) $\gamma_{sv} = \gamma_{ls} + \gamma_{lv} \cos\theta_Y$
137 where θ_Y is the Young contact angle at the air/liquid/solid junction.
138 The work of adhesion, W_a and the spreading coefficient, S_{ls} can be calculated as follows:

(2) $W_a = \gamma_{sv} + \gamma_{lv} - \gamma_{ls}$

(3) $S_{ls} = \gamma_{sv} - \gamma_{lv} - \gamma_{ls}$

If S_{ls} is positive, spreading will occur spontaneously. As θ_Y is finite, S_{ls} is always negative and if the contact angle is zero, complete wetting/spreading occurs [24].

Static contact angle analyses were performed using Krüss Easy Drop instrument. Milli-Q water, diethylene glycol, ethylene glycol, diiodomethane and ethylene glycol/water 50% v/v mixture were adopted for the determination of the Surface Free Energy (SFE) or solid-vapor surface tension (γ_{sv}) of the tested molds, using the Owens, Wendt, Rabel and Kaeble (OWRK) method [25]. Wetting Envelopes (WEs) were elaborated starting from the previous data [26].

Potentiodynamic polarizations were performed to study the corrosion capacity of the optimized emulsion towards aluminum molds. An AMEL Saturated Calomel Electrode (SCE) and a Metrohm platinum electrode were used as reference and counter electrodes, respectively. The working electrode was prepared by embedding aluminum sample in epoxy resin to guarantee the same surface exposition (around 1.5 cm^2). Before every anodic polarization, the Al-alloy sample was sanded with 1200 grit sandpaper until no pits were visible. The sample was then immersed into a 100 cm^3 jacketed glass cell (maintained at 25°C), containing 90 g of 5% w/w emulsion or acetic acid solution (as reference sample at the same emulsion pH). A starting cathodic chronoamperometric analysis was used to remove all aluminum passivation products. This measure was performed at –2.5 V *vs* SCE under stirring condition for 750 s. Then, the OPC determination was carried out for 120 s and the starting and stop potentials were set to –1.5 V and +2.0 V *vs* OCP, respectively. The polarization tests (by Autolab PGSTAT101 potentiostat/galvanostat equipped with Nova 1.11 software) were conducted using a scan rate of 1 mV s^{-1}.

Scanning Electron Microscopy analyses (SEM HITACHI TM-1000) were performed on aluminum samples before and after the potentiodynamic polarization experiments.

3. Results and Discussion

3.1 O/W emulsions optimization and chemometric analysis

All the O/W formulations were prepared by inversion point emulsification (see the "Wax-based O/W emulsions" paragraph). By exploiting this particular method, a great viscosity variation is usually observed

since, at the beginning, hot water is slowly dripped onto the oil phase under vigorous stirring thus leading to an increase of the system viscosity. Then, after the addition of the majority of water, the system passes through the inversion point and a viscosity collapse occurs.

Several oil-in-water emulsions (33 samples) were formulated by modulating both physical parameters, *i.e.* time of water addition (28-95 min), emulsification stirring (200-320 rpm), cooling rate (0.2-1.4 °C min^{-1}) and stirring (100-210 rpm), and chemical composition such as water hardness (2, 15 and 250 μS cm^{-1}), acetic acid (0.6-3.1%), alcohol (0.8-1.4%) and amine (1.0-2.1%) amounts. To investigate the emulsions stability, average droplet sizes together with the flocs percentage (by DLS and microscope measurements), destabilization heights and clarification/creaming phenomena (by Turbiscan) were determined (Table 2, Figures 3 and S2). Since many objects were described by many variables (Table 2), the use of PCA analysis was mandatory. Figures 1a (PC2 *vs* PC1) and 1b (PC3 *vs* PC1) show the loading plots calculated considering the first three principal components. Thus, we could observe: *i*) a poor correlation between physical and chemical parameters, *ii*) the destabilization particularly increases by increasing the droplets size ($<d^{DLS}>$ parameter) and water conductivity, *iii*) flocs percentage grows with the decreasing of both amine/alcohol amounts and stirring rate during the emulsification process. Figure 1b corroborates the previous observations. In addition, here the cooling rate parameter seems to be correlated with flocs percentage. Indeed, the faster the cooling rate (higher than 0.3-0.5 °C min^{-1}), the greater the emulsion destabilization. Moreover, in both loading plots the percentage of acetic acid does not seem to be correlated with the flocs percentage.

Specifically, starting from $E\_N_{1.5}Cet_{1.0}Ac_{3.1}$ sample (Table 2, reference sample), the aforementioned physical variables were modified (2^{nd}-4^{th} columns, bold data), obtaining 19 different formulations. The variation of both the time of water addition and the stirring rate are crucial parameters for the formation of a stable emulsion, since the emulsification process implies the use of high energy to brake the disperse phase into smaller and smaller droplets. These two variables were directly proportional and, if insufficient stirring rate (lower than 320 rpm during emulsification) was adopted or water excess was added in a very short period of time, two separate bulk phases began to appear. Moreover, in high stirring rate conditions (>320 rpm, sample 17), a destabilization effect occurred since oil droplets began to merge. Alongside the emulsification stirring, the cooling one should be 130-140 rpm to maintain constant the droplets size

195 distribution. Hence, taking into account both the DLS results (Table 2, 11th column, *i.e.* the lower the
196 droplets size and the relative standard deviations, the more stable the emulsions) and the flocs percentages
197 (Table 2, 12th column), we assumed that the optimal conditions should be: *i*) a time of water addition of
198 around 70-90 minutes, *ii*) a high stirring rate during the emulsification process (320 rpm) and *iii*) a low
199 stirring rate during the cooling step (135 rpm). Furthermore, in the literature [20,27], it is reported that a fast
200 cooling rate promotes emulsion stability. However, if it is too fast, the opposite undesired effect will be
201 obtained. For this reason, several tests were performed by varying the cooling rate (Table 2 and Figure 2)
202 and we observed that destabilization phenomena could occur (*i.e.* a pearled effect was noticed, due to the
203 amine tenside desorption from the oil phase [28]) when either lower (0.2 °C min^{-1}, Fig. 2 curve 6) or higher
204 (above 0.8 °C min^{-1}, Fig. 2 curves 1, 2 and 5) rate values were adopted. Hence, we assumed the rate of 0.3-
205 0.5 °C min^{-1} as the optimum to be subsequently used (Fig. 2, curves 3-4).

206 Once obtained the most suitable experimental set-up, chemical composition was varied (Table 2,
207 samples 19-33, bold italic data). The effect of water conductivity has been studied by adopting three types of
208 water sample (see Table 2, 6th column; samples 19, 20 and 22). In this case, the destabilization height
209 parameter showed that the higher the water conductivity, the lower the emulsion stability (Table 2, 13th
210 column). Indeed, the water electrolytes can compensate the net charge present on the oil droplets surface,
211 reducing the double layer and thus favoring coalescence and Ostwald ripening phenomena. This effect was
212 further confirmed by measuring the DLS average droplets size (Table 2, 11th column) and backscattering
213 analyses, in which a wider clarification phenomenon was observed over time (Figure 3a). Actually,
214 emulsions formulated by using Milli-Q water showed either a lower presence of bigger droplets population
215 (~400-700 *vs* >1000 nm) or the absence of flocs (Table 2, 12th column).

216 Subsequently keeping constant Milli-Q water, the acetic acid, amine and cetyl alcohol
217 concentrations, which represent the crucial experimental variables, were progressively varied. To ensure
218 emulsions formation and stabilization, the presence of acetic acid (acting as solubilizer) is mandatory. Since
219 fatty amine has a very low HLB value, its solubility in water is very limited. Indeed, at neutral and acidic
220 conditions, the amine is positively charged: the presence of a counterion can make it more water soluble.
221 However, this counterion should not be so big since destabilization could occur due to incompatibility
222 between anionic and cationic species, and it should not be an inorganic acid due to subsequent corrosion

problems. Therefore, acetic acid (representing a good compromise) was studied in different concentrations, ranging from 0.6% to 3.1% (Table 2, 7th column, samples 22-25). Particularly, if its amount is too low, the emulsions became less stable (higher <d^{DLS}> values and destabilization heights; Table 2, 11th-13th columns) and a solid amine precipitated during the emulsification process. Nevertheless, its excessive concentration could lead to a destabilization effect caused by the double layer compression. Also, as expected, the pH values of the prepared emulsions (Table 2, 10th column) varied modulating the acid percentage. Under these considerations, 2.5% turned out to be the most suitable concentration in terms of higher stability and smaller oil droplets size. Then, the amine/surfactant percentage was modified in the range 1.0% - 2.1%, starting from the initial E_$N_{1.5}Cet_{1.0}Ac_{3.1}$ (Table 2, sample 22, in which it was 1.5%). The amine concentration plays a pivotal role in affecting both the droplets size and the emulsions stability, since it is the main emulsifier. A drastic decrease of the amine amount (down to 1.0%, sample 27) led to a destabilization effect, corroborated by the increasing of droplets dimensions (Table 2, 11th column), and the observation of a blurry line separation in Abbe refractometer. On the contrary, a too high percentage (*i.e.* 2.1%, sample 29) seemed to slightly destabilize the system, because a little increase of <d^{DLS}> values and the occurrence of clarification/creaming effects (Figures 3b and S2) have been observed. Hence, 1.8% has been chosen as the optimal amine amount (Fig. 3c). Finally, as the last investigated ingredient, cetyl alcohol (used as the co-surfactant) concentration was varied between 0.8% and 1.4% (samples 28, 31-33). We noticed that alcohol amount did not deeply affect the emulsions stability, but only a less decrease of droplets dimension was appreciable either for lower or higher values than 1.2%.

Hence, by evaluating both the experimental and the PCA results, the optimized emulsion turned out to be E_$N_{1.8}Cet_{1.2}Ac_{2.5}$. This emulsion, contrarily to the initial one, showed a net line separation in the Abbe refractometer (Fig. S3), a lower destabilization along with smaller oil droplets (Table 2, sample 33).

Aging experiments were further carried out to investigate its long-term stability. DLS granulometric size distribution under aging conditions (after 1, 2, 3 and 4 weeks) for both E_$N_{1.5}Cet_{1.0}Ac_{3.1}$ and E_$N_{1.8}Cet_{1.2}Ac_{2.5}$ emulsions are shown in Figure 4. The droplets size passed from ~900 nm to over 1 μm for the reference emulsion (sample 1, Fig. 4a), whereas the optimized one showed a negligible variation of the <d^{DLS}> (from ~500 to ~900 nm, Fig. 4b). Therefore, the final product, obtained by varying both the physical and chemical parameters, revealed to be stable even on the long-term period.

3.2 Optimized emulsion/mold interactions

All the prepared emulsions should be adopted as releasing agent to be applied on different types of mold substrates (*e.g.* aluminum, polyester and epoxy resin). For this purpose, their wettability features were evaluated measuring the contact angles with different solvents (see the Materials and methods section). The surface free energy values together with their polar and disperse components can be extrapolated by adopting the linear fitting OWRK function [25] (Figure 5). Both the organic-based materials (polyester and epoxy resins) and the metal substrates (those sonicated in 2-propanol, to reproduce working conditions) are characterized by similar SFE values (Table in inset Fig. 5), whose polar component is lower than 10 mN m^{-1}. In the case of the aluminum mold, a further treatment by chemical etching (5% hot oxalic acid) was carried out to achieve a cleaner surface. This step made the surface more hydrophilic leading to a SFE value of around 53 mN m^{-1}, with a polar component four times higher than the pristine one. The present behaviour was also corroborated by studying the relative Wetting Envelopes [26] (WEs, Figure S4), in which bow-shaped curves represent the wettability features of the Al substrate by liquids, whose polar and disperse components lie in the θ-wetting area. Hence, the higher hydrophilicity of chemically etched aluminum is evidenced by the swollen of the bow-lines; this fact implies that the water solvent wets better the surface since the contact angle shifts from 75° (Fig. S4a) to 41° (Fig. S4b).

After having measured the surface tension of the optimized E_$N_{1.8}Cet_{1.2}Ac_{2.5}$ (γ_{lv} = 30 mN m^{-1}), the work of adhesion (W_a) and the spreading coefficient (S_{ls}) were calculated (Table 3). Similar results were obtained adopting both the organic and metal substrates; these experimental data suggested a desired wettability towards the adopted emulsion. Thus, all the three materials can be used indifferently for PUs molding. On the contrary, in the case of etched aluminum, its more hydrophilic nature led to a poor interaction with the tested emulsion.

3.3 Optimized emulsion corrosion properties

Since aluminum was one of the adopted mold, polarization tests have been performed to evaluate the corrosiveness of the optimized emulsion (Fig. 6). In the present case, localized attack such as pitting phenomena could produce general corrosion [29]. Hence, the optimized formulation was tested and the

corrosion potential (E_{corr}) was compared to value obtained by using a solution of acetic acid (at the same pH of the optimized emulsion), used as reference sample. As reported in Table in the inset of Figure 6, the acetic acid polarization curve showed a more noble E_{corr} (-0.41 *vs* -0.81 V). Moreover, the higher current density values for acetic acid underline the presence of higher corrosion rate. This confirms that the optimized emulsion has inhibition properties thanks to the presence of both fatty amine and oil phase. Indeed, it is widely reported that amines, being adsorbed onto metal substrates, prevent them from corrosion [23,30–32]. Furthermore, by observing the shape of the polarization curves, the formation of a passivation film and its subsequent break could be hypothesized only in the case of emulsion test. Indeed, in the anodic branch (at potentials over +0.45 V), a sharp increase of the current density values can be noticed, representing the starting of pits formation.

These corrosion phenomena were also observed by scanning electron microscopy (Fig. S5). Corroded sample (Fig. S5b) showed the presence of several pits on the whole surface, which were absent in the pristine aluminum mold (Fig. S5a).

4. Conclusions

In the present study, several wax-based O/W emulsions were prepared in a 2 L pilot plant to be used as release agent for PU solid foams. However, the formulation of emulsions with optimal removal features, high stability during storage, low corrosiveness and good environmental compatibility is nowadays a challenging issue. Actually, few patents [6,10,12,16,18] and a scarce number of scientific reports [19,22] are available so far.

By analyzing data obtained varying both physical and chemical variables of the starting emulsion, we succeeded in preparing an optimal product that showed good performances in terms of stability, low corrosion phenomena and optimal spreading behaviour (either on aluminum or polyester/epoxy molds). Moreover, due to the increasing complexity of the system, Principal Component Analysis were carried out to find the best correlations among all the investigated variables and to have some predictions on the role of the different raw materials in affecting the final stability of the emulsions.

At first, physical parameters were varied and optimal emulsification conditions were found, *i.e.* time of water addition of ~70-90 minutes, high stirring rate during the emulsification process (320 rpm), low

307 during the cooling step (135 rpm), and cooling rate of 0.3-0.5 °C min^{-1}. Subsequently, chemical composition
308 (such as type of water, acetic acid, amine and alcohol concentrations) was optimized. Specifically,
309 E_$N_{1.8}Cet_{1.2}Ac_{2.5}$ sample represented the most performing one in terms of low droplets size, lower
310 destabilization with the increasing of temperature and higher long-term stability.

311 Afterwards, the interaction between the optimized emulsion and different types of molds was
312 studied. Since both the substrates possess similar SFE values (with polar component lower than 10 mN m^{-1})
313 and the surface tension of the optimized E_$N_{1.8}Cet_{1.2}Ac_{2.5}$ was equal to 30 mN m^{-1}, the work of adhesion and
314 the spreading coefficient values suggested a desired wettability towards the adopted emulsion.

315 Furthermore, releasing agents should not cause corrosion phenomena in the case of metal-based
316 molds. Therefore, electrochemical anodic polarization measurements were carried out. The presence of either
317 amine or oil phase hindered pits formation on aluminum surface with respect to pure acetic acid. However,
318 higher potentials could break the passivation film, thus leading to pitting corrosion observed by electron
319 microscopy.

320 Hence, the present work succeeded in formulating an optimal O/W releasing agent to be applied in
321 the field of PUs solid foams molding.

322

323 **Acknowledgements**

324 Gruppo Italiano di Chemiometria is gratefully acknowledged for the chemometric software and helpful
325 training.

326 Conflict of Interest: The authors declare that they have no conflict of interest.

References

[1] G. Li, L. Dong, Z. Bai, M. Lei, J. Du, Predicting carbonation depth for concrete with organic film coatings combined with ageing effects, Constr. Build. Mater. 142 (2017) 59–65. doi:10.1016/j.conbuildmat.2017.03.063.

[2] S.H. Kim, H.C. Park, H.M. Jeong, B.K. Kim, Glass fiber reinforced rigid polyurethane foams, J. Mater. Sci. 45 (2010) 2675–2680. doi:10.1007/s10853-010-4248-3.

[3] E. Kabakci, G. Sayer, E. Suvaci, O. Uysal, İ. Güler, M. Kaya, Processing-structure-property relationship in rigid polyurethane foams, J. Appl. Polym. Sci. 134 (2017) 1–13. doi:10.1002/app.44870.

[4] F. Beshkar, H. Khojasteh, M. Salavati-Niasari, Recyclable magnetic superhydrophobic straw soot sponge for highly efficient oil/water separation, J. Colloid Interface Sci. 497 (2017) 57–65. doi:10.1016/j.jcis.2017.02.016.

[5] K. Choupani Chaydarreh, A. Shalbafan, J. Welling, Effect of ingredient ratios of rigid polyurethane foam on foam core panels properties, J. Appl. Polym. Sci. 134 (2017) 1–8. doi:10.1002/app.44722.

[6] H. Ralf Althoff, T. Henning, W. Helmut Lammerting, Aqueous release agent and its use in the production of polyurethane moldings, US 2007/0110840 A1, 2007.

[7] L. Figueiredo, P. Bandeira, A. Mendes, M.M.S.M. Bastos, F.D. Magalhães, Use of fluoropolymer permanent release coatings for molded polyurethane foam production, J. Coatings Technol. Res. 9 (2012) 757–764. doi:10.1007/s11998-012-9413-y.

[8] J. Blahak, H. Menk, Release agent for removing polyurethane plastic from molds, 4,312,672, 1982.

[9] Z. Li, Z. Lu, W. Xing, L. Bao, P. Wang, J. Xu, Y. Zhang, A release agent, the preparation and use thereof, WO 2012/104346 Al, 2012.

[10] T. Hattich, G. Schuster, Release agent for urethane foam molding, 4,969,952, 1990.

[11] R.J. Wesala, Mold Release Agents and Means of Application, 4,491,607, 1985.

[12] H. Ralf Althoff, S. Torsten Henning, W. Helmut Lammerting, Aqueous release agent and its use in the production of polyurethane moldings, US 8,748,514 B2, 2014.

[13] M.E. Harakal, G.J. Wasilczyk, G.D. Andrew, M. Scarpati, Z. Makus, Water based mold release compositions containing poly(siloxane-giycol) surfactants for making polyurethane foam article in a

mold, 89112755.7, 1991.

[14] R. Cited, O. City, R.U.A. Data, (12) United States Patent, 1 (2003) 0–4. doi:10.1016/j.(73).

[15] M.P. Aronson, The role of free surfactant in destabilizing oil-in-water emulsions, Langmuir. 5 (1989) 494–501. doi:10.1021/la00086a036.

[16] A. Schneider, V. Schneider, H. Wochnowski, P. Niemeyer, Release agent, 6,162,290, 2000.

[17] M.E. Cekoric, R.M. Loring, W.A. Ludwico, Talc based external mold release agent for polyurethane foams, 4,131,662, 1978.

[18] T. Henning, Solvent-free release agent and its use in the production of polyurethane moldings, US 2009/0020917 A1, 2009.

[19] A. Cambiella, J.M. Benito, C. Pazos, J. Coca, M. Ratoi, H. a. Spikes, The effect of emulsifier concentration on the lubricating properties of oil-in-water emulsions, Tribol. Lett. 22 (2006) 53–65. doi:10.1007/s11249-006-9072-1.

[20] C. Li, Z. Mei, Q. Liu, J. Wang, J. Xu, D. Sun, Formation and properties of paraffin wax submicron emulsions prepared by the emulsion inversion point method, Colloids Surfaces A Physicochem. Eng. Asp. 356 (2010) 71–77. doi:10.1016/j.colsurfa.2009.12.036.

[21] A. Cambiella, J.M. Benito, C. Pazos, J. Coca, Interfacial properties of oil-in-water emulsions designed to be used as metalworking fluids, Colloids Surfaces A Physicochem. Eng. Asp. 305 (2007) 112–119. doi:10.1016/j.colsurfa.2007.04.049.

[22] J.M. Benito, A. Cambiella, A. Lobo, G. Gutiérrez, J. Coca, C. Pazos, Formulation, characterization and treatment of metalworking oil-in-water emulsions, Clean Technol. Environ. Policy. 12 (2010) 31–41. doi:10.1007/s10098-009-0219-2.

[23] A. Lotierzo, V. Pifferi, S. Ardizzone, P. Pasqualin, G. Cappelletti, Insight into the role of amines in Metal Working Fluids, Corros. Sci. 110 (2016) 192–199. doi:10.1016/j.corsci.2016.04.028.

[24] M.J. Rosen, Wetting and its modification by surfactants, in: Surfactants Interfacial Phenom, John Wiley & Sons Inc., 1978: pp. 174–199.

[25] D.K. Owens, R.C. Wendt, Estimation of the surface free energy of polymers, J. Appl. Polym. Sci. 13 (1969) 1741–1747.

[26] G. Cappelletti, S. Ardizzone, D. Meroni, G. Soliveri, M. Ceotto, C. Biaggi, M. Benaglia, L.

Raimondi, Wettability of bare and fluorinated silanes: A combined approach based on surface free energy evaluations and dipole moment calculations, J. Colloid Interface Sci. 389 (2013) 284–291. doi:10.1016/j.jcis.2012.09.008.

[27] H. Mollet, A. Grubernmann, Formulation Technology, 2001.

[28] T.F. Tadros, Dispersion of Powders Rheology of Dispersions Self-Organized Surfactant Structures and Particles Colloids and Interface Science Series, n.d.

[29] A. Von Hehl, K. Peter, Aluminum and aluminum alloys, Struct. Mater. Process. Transp. (2013) 49–99.

[30] J. Buchweishaija, Corrosion Inhibiton of Carbon Steel by an Amine-Fatty Acid in Acidic Solution, Tanzania J. Sci. 29 (2002) 99–108.

[31] M. a. Migahed, M. Abd-El-Raouf, a. M. Al-Sabagh, H.M. Abd-El-Bary, Corrosion inhibition of carbon steel in acid chloride solution using ethoxylated fatty alkyl amine surfactants, J. Appl. Electrochem. 36 (2006) 395–402. doi:10.1007/s10800-005-9094-7.

[32] J. de Damborenea, J.M. Bastidas, A.J. Vázquez, Adsorption and inhibitive properties of four primary aliphatic amines on mild steel in 2 M hydrochloric acid, Electrochim. Acta. 42 (1997) 455–459. doi:10.1016/S0013-4686(96)00250-2.

400 **Table 1.** Emulsion general composition.

401

Ingredients	%
Water	≤ 90.0
Wax	≤ 2.0
Organic solvent	8.5 – 10.0
Silicones	0.7 – 1.1
Cetyl alcohol	≤ 1.4
Linear Fatty amine	≤ 2.1
Acetic acid	0.6 – 3.1
Other ingredients: antioxidants, preservatives	0.1 – 0.5

402

Table 2. Investigated physical/chemical variables and results obtained by means of both Dynamic Light Scattering analysis (standard deviations upon ten repetitions have been also reported) and emulsion destabilization height evaluation. Bold samples: variation of physical parameters; bold italic data: variation of chemical composition.

Sample	Physical variables				Chemical variables					Physico-chemical results		
	H_2O addition / min	Emulsification stirring / rpm	Cooling stirring / rpm	Cooling rate / °C min^{-1}	H_2O conductivity / µS cm^{-1}	% Acetic acid	% Amine	% Alcohol	pH	$<d^{DLS}>$ / nm	% Flocs	Destabilization
1	**55**	**220**	**200**	**0.8**	250	3.1	1.5	1.0	3.3	1400 ± 500	2	0.47
2	**30**	**200**	**100**	**0.8**	250	3.1	1.5	1.0	3.3	1200 ± 400	11	0.47
3	**57**	**200**	**100**	**0.8**	250	3.1	1.5	1.0	3.3	1500 ± 600	14	0.63
4	**55**	**200**	**100**	**0.8**	250	3.1	1.5	1.0	3.3	1500 ± 300	34	0.47
5	**28**	**200**	**100**	**0.3**	250	3.1	1.5	1.0	3.3	1200 ± 400	9	0.47
6	**33**	**200**	**100**	**0.3**	250	3.1	1.5	1.0	3.3	1200 ± 400	7	0.49
7	**35**	**200**	**100**	**0.3**	250	3.1	1.5	1.0	3.3	900 ± 400	11	0.49
8	**35**	**200**	**100**	**0.3**	250	3.1	1.5	1.0	3.3	1200 ± 300	8	0.50
9	**28**	**200**	**100**	**0.2**	250	3.1	1.5	1.0	3.3	1100 ± 400	9	0.63
10	**31**	**200**	**100**	**0.2**	250	3.1	1.5	1.0	3.3	1200 ± 400	17	0.54
11	**53**	**200**	**100**	**0.2**	250	3.1	1.5	1.0	3.3	1200 ± 300	13	0.51
12	**70**	**200**	**100**	**0.5**	250	3.1	1.5	1.0	3.3	1400 ± 600	4	0.49
13	**40**	**200**	**100**	**0.5**	250	3.1	1.5	1.0	3.3	1000 ± 400	2	0.49
14	**40**	**240**	**120**	**0.5**	250	3.1	1.5	1.0	3.3	1000 ± 400	9	0.50
15	**33**	**300**	**135**	**1.0**	250	3.1	1.5	1.0	3.3	1200 ± 400	1	0.54
16	**33**	**300**	**210**	**1.4**	250	3.1	1.5	1.0	3.3	1500 ± 500	2	0.57
17	**44**	**350**	**135**	**0.8**	250	3.1	1.5	1.0	3.3	1000 ± 300	3	0.54
18	**45**	**320**	**135**	**0.8**	250	3.1	1.5	1.0	3.3	1200 ± 200	3	0.50
19	**80**	**320**	**135**	**0.5**	***250***	***3.1***	***1.5***	***1.0***	3.3	1000 ± 200	1	0.46
20	75	320	135	0.5	***15***	***3.1***	***1.5***	***1.0***	3.3	700 ± 400	4	0.09
21	80	320	135	0.5	***15***	***2.5***	***1.5***	***1.0***	3.5	800 ± 400	0	0.20
22	78	320	135	0.5	***2***	***3.1***	***1.5***	***1.0***	3.3	500 ± 200	0	0.04
23	88	320	135	0.5	***2***	***1.5***	***1.5***	***1.0***	3.9	1000 ± 500	5	0.29
24	78	320	135	0.5	***2***	***1.0***	***1.5***	***1.0***	4.2	900 ± 400	7	0.14
25	95	320	135	0.5	***2***	***0.6***	***1.5***	***1.0***	4.6	800 ± 400	4	0.21
26	80	320	135	0.5	***2***	***2.5***	***1.5***	***1.0***	3.4	400 ± 200	0	0.04
27	77	320	135	0.5	***2***	***2.5***	***1.0***	***1.0***	4.0	700 ± 400	3	0.21
28	80	320	135	0.5	***2***	***2.5***	***1.8***	***1.0***	4.0	500 ± 300	0	0.03
29	84	320	135	0.5	***2***	***2.5***	***2.1***	***1.0***	3.3	500 ± 400	0	0.04
30	78	320	135	0.5	***2***	***2.5***	***1.5***	***1.2***	3.3	380 ± 90	0	0.04
31	81	320	135	0.5	***2***	***2.5***	***1.8***	***0.8***	3.4	500 ± 200	0	0.04
32	80	320	135	0.5	***2***	***2.5***	***1.8***	***1.4***	3.6	500 ± 100	0	0.04
33	90	320	135	0.5	***2***	***2.5***	***1.8***	***1.2***	3.4	350 ± 70	0	0.04

407 **Table 3.** Contact angle values and wetting parameters (work of adhesion, W_a and spreading coefficient, S_{ls})
408 for the optimized emulsion (γ_{lv} = 30 ± 1 mN m^{-1}).
409
410
411
412

Sample	E_$N_{1.8}Cet_{1.2}Ac_{2.5}$		
	Aluminum	**Polyester mold**	**Epoxy mold**
θ / deg	64 ± 2	56 ± 3	53 ± 2
W_a / mN m^{-1}	43 ± 2	47 ± 3	48 ± 2
S_{ls} / mN m^{-1}	-(17 ± 2)	-(13 ± 3)	-(12 ± 2)

Figure captions

Figure 1. Loading plot of **a)** PC2 *vs* PC1and **b)** PC3 *vs* PC1 for a total of explained variance of around 60% for both cases.

Figure 2. Reactor temperature variations as a function of time (cooling rate) together with relative emulsion photos.

Figure 3. Backscattering analysis of different emulsions in the case of: **a)** osmotized water; **b)** highest amine concentration (2.1%); **c)** optimized formulation. Inset: corresponding optical microscope images at 400x magnification.

Figure 4. DLS granulometric size distribution after 1, 2, 3 and 4 weeks of aging in the case of **a)** E_$N_{1.5}Cet_{1.0}Ac_{3.1}$ and **b)** E_$N_{1.8}Cet_{1.2}Ac_{2.5}$ emulsions.

Figure 5. SFE elaboration for the aluminum, polyester and epoxy resin substrates. Table in inset: total SFE (γ_s) and its relative polar (γ_s^p) and disperse (γ_s^d) components.

Figure 6. Polarization curves of acetic acid (pH 4, reference sample) and O/W optimized emulsion (namely E_$N_{1.8}Cet_{1.2}Ac_{2.5}$). Table in inset: corrosion potential (E_{corr}) values.

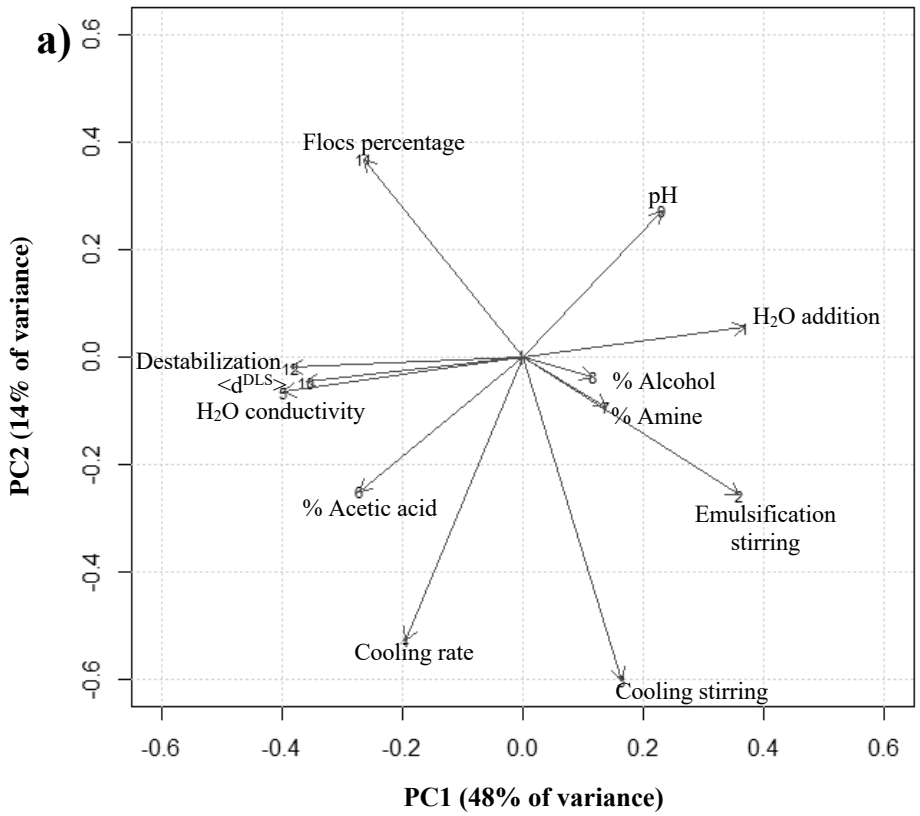
a)
Flocs percentage
pH
H2O addition
Destabilization
<dDLS>
H2O conductivity
% Alcohol
% Amine
% Acetic acid
Emulsification stirring
Cooling rate
Cooling stirring
PC2 (14% of variance)
PC1 (48% of variance)
-0.6
-0.4
-0.2
0.0
0.2
0.4
0.6

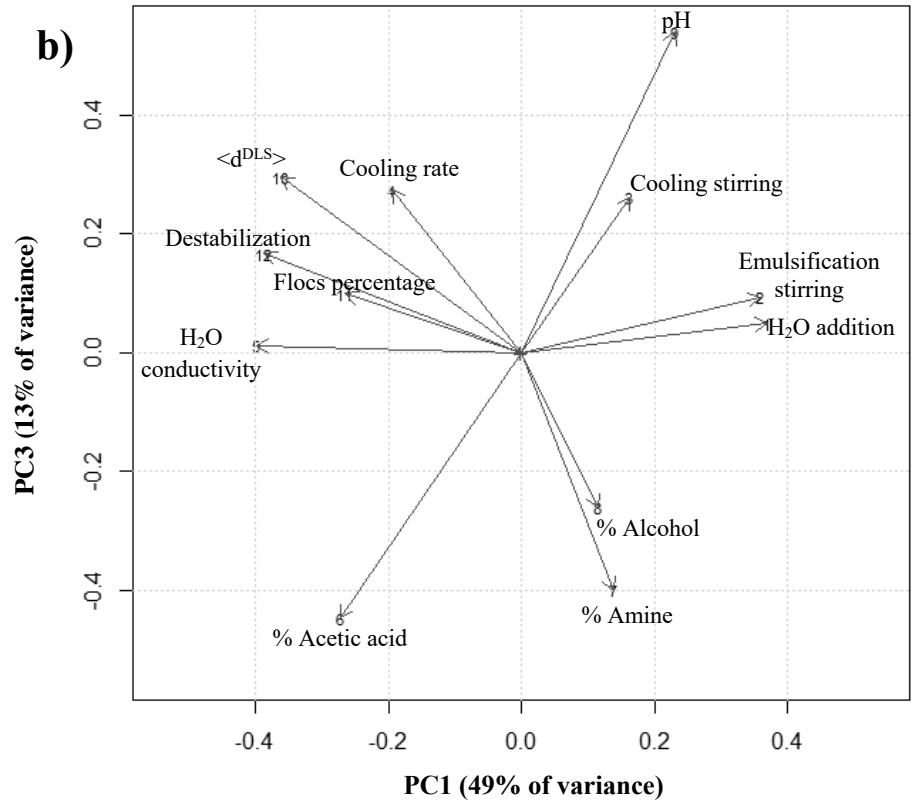
b)
pH
<dDLS>
Cooling rate
Cooling stirring
Destabilization
Flocs percentage
Emulsification stirring
H2O addition
H2O conductivity
% Alcohol
% Amine
% Acetic acid
PC3 (13% of variance)
PC1 (49% of variance)
-0.4
-0.2
0.0
0.2
0.4

FIGURE 1

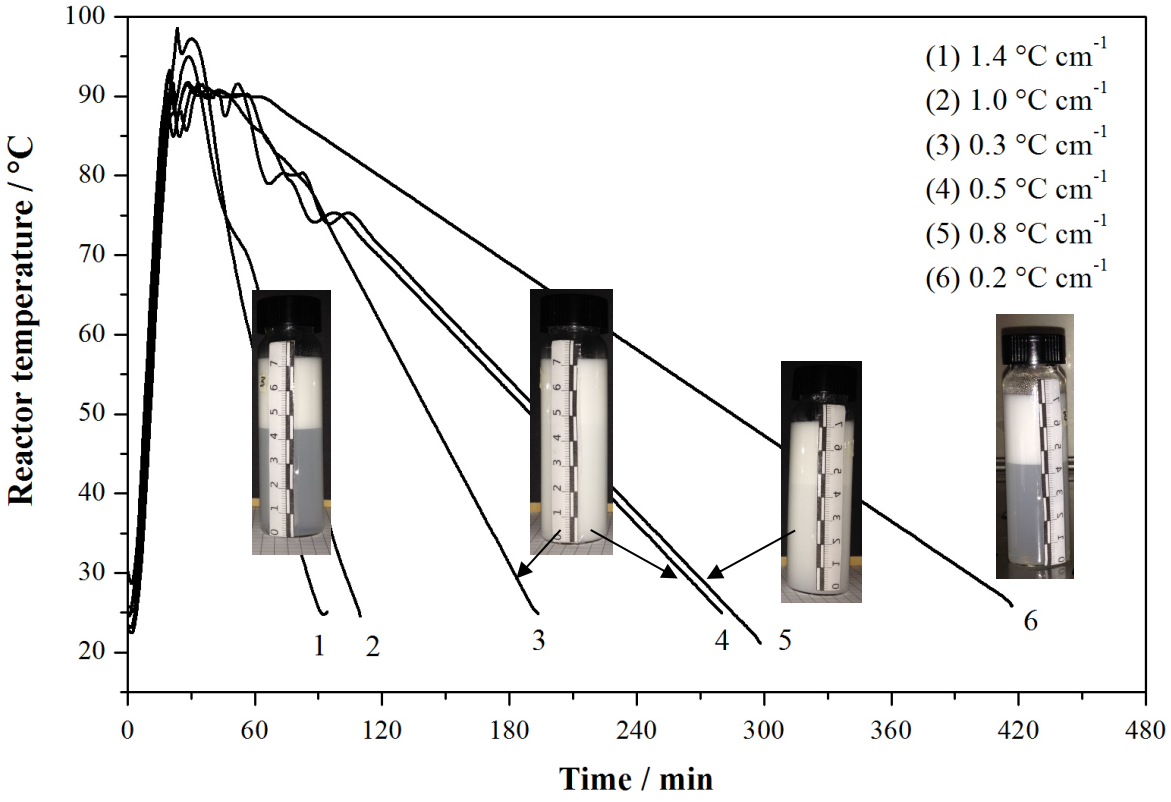

461

462

463

464 **FIGURE 2**

465

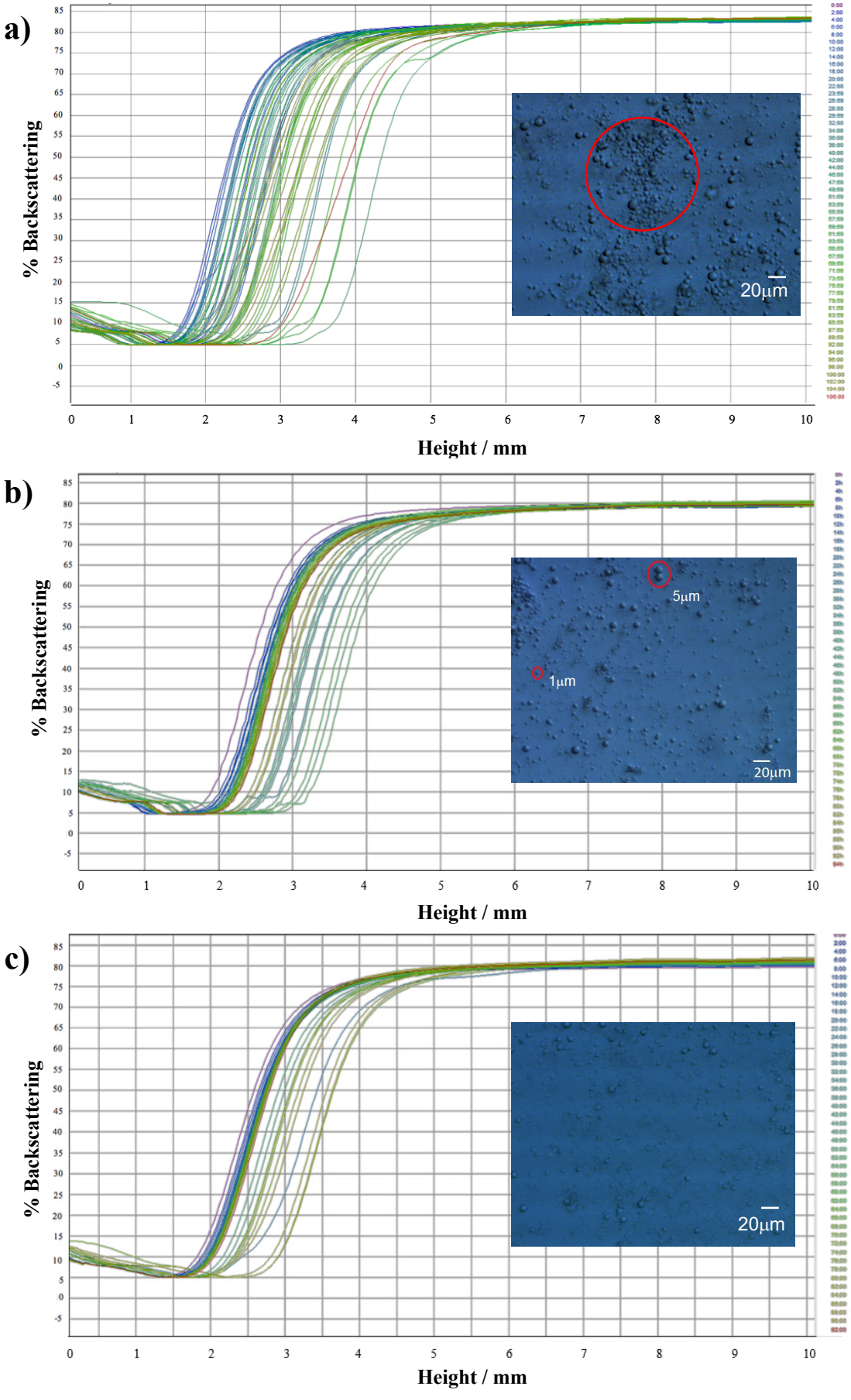
a)
% Backscattering
Height / mm
20µm
b)
% Backscattering
Height / mm
5µm
1µm
20µm
c)
% Backscattering
Height / mm
20µm

FIGURE 3

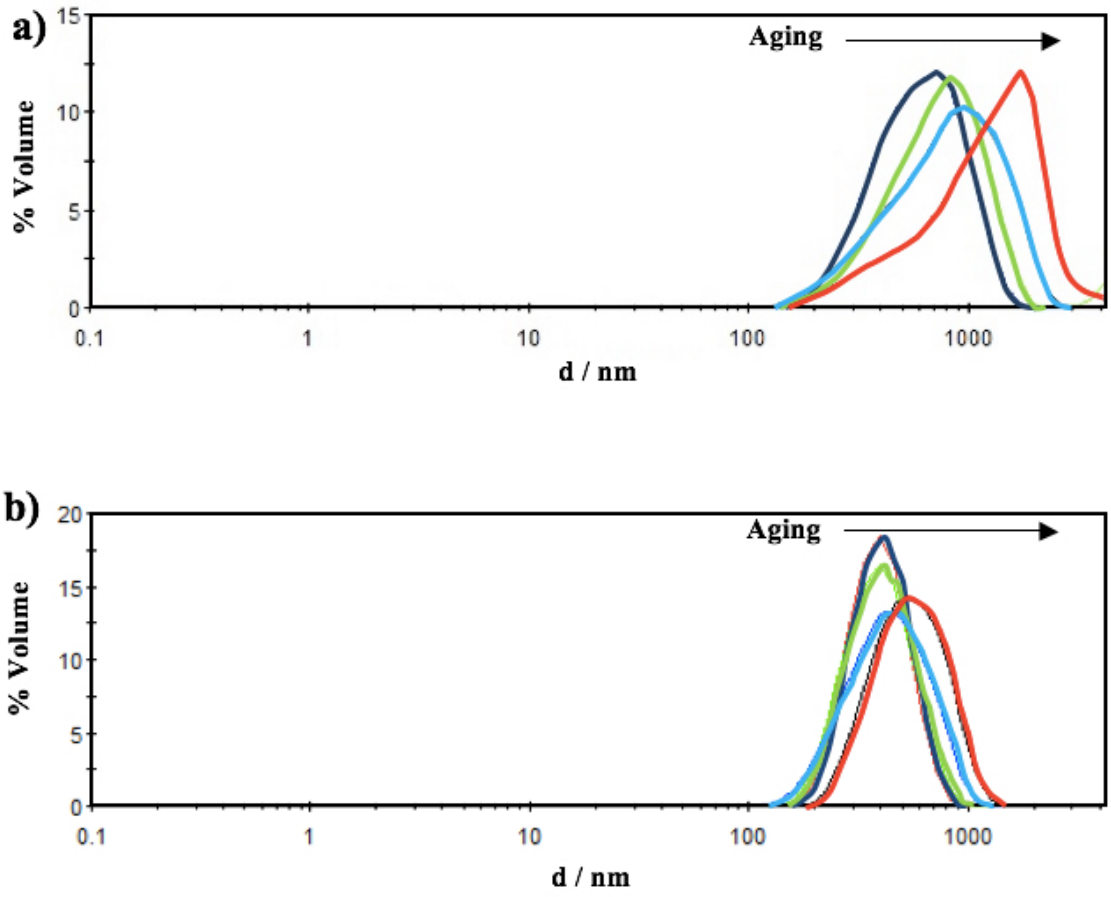
a)
Aging
% Volume
15
10
5
0
0.1
1
10
100
1000
d / nm
b)
Aging
% Volume
20
15
10
5
0
0.1
1
10
100
1000
d / nm

FIGURE 4

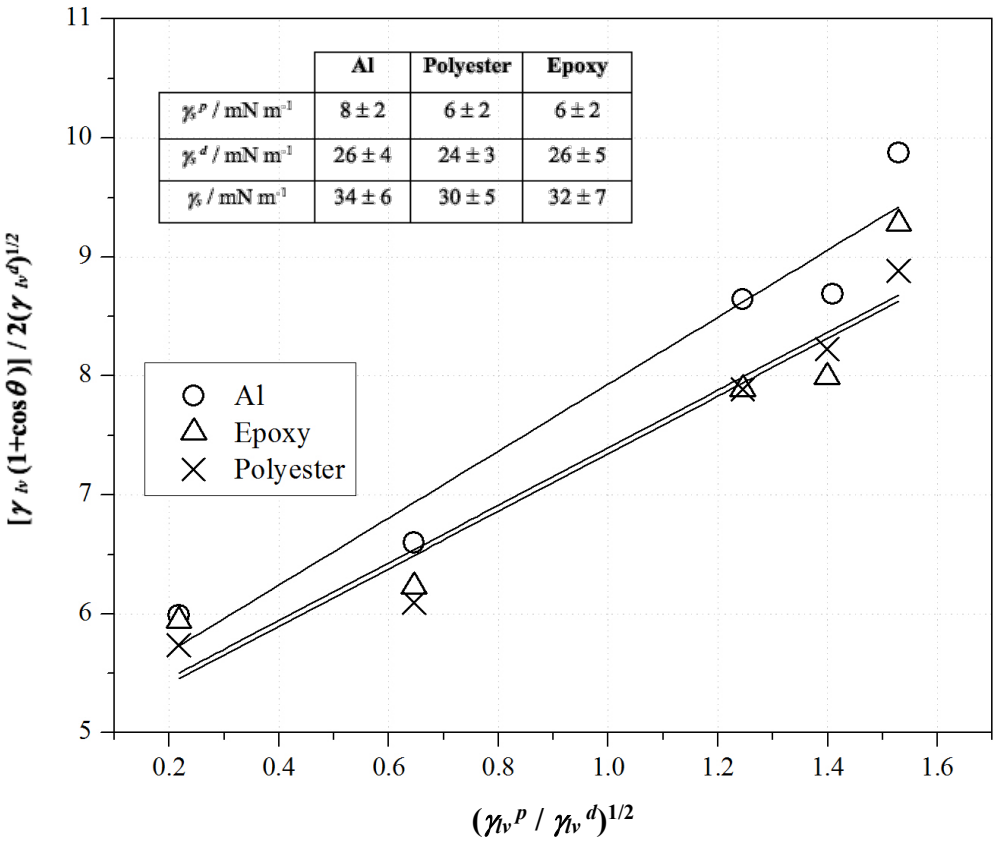
Al
Polyester
Epoxy
γ_s^p / mN m^{-1}
8 ± 2
6 ± 2
6 ± 2
γ_s^d / mN m^{-1}
26 ± 4
24 ± 3
26 ± 5
γ_s / mN m^{-1}
34 ± 6
30 ± 5
32 ± 7
Al
Epoxy
Polyester
$[\gamma_{lv}(1+\cos\theta)] / 2(\gamma_{lv}^d)^{1/2}$
$(\gamma_v^p / \gamma_v^d)^{1/2}$
11
10
9
8
7
6
5
0.2
0.4
0.6
0.8
1.0
1.2
1.4
1.6

FIGURE 5

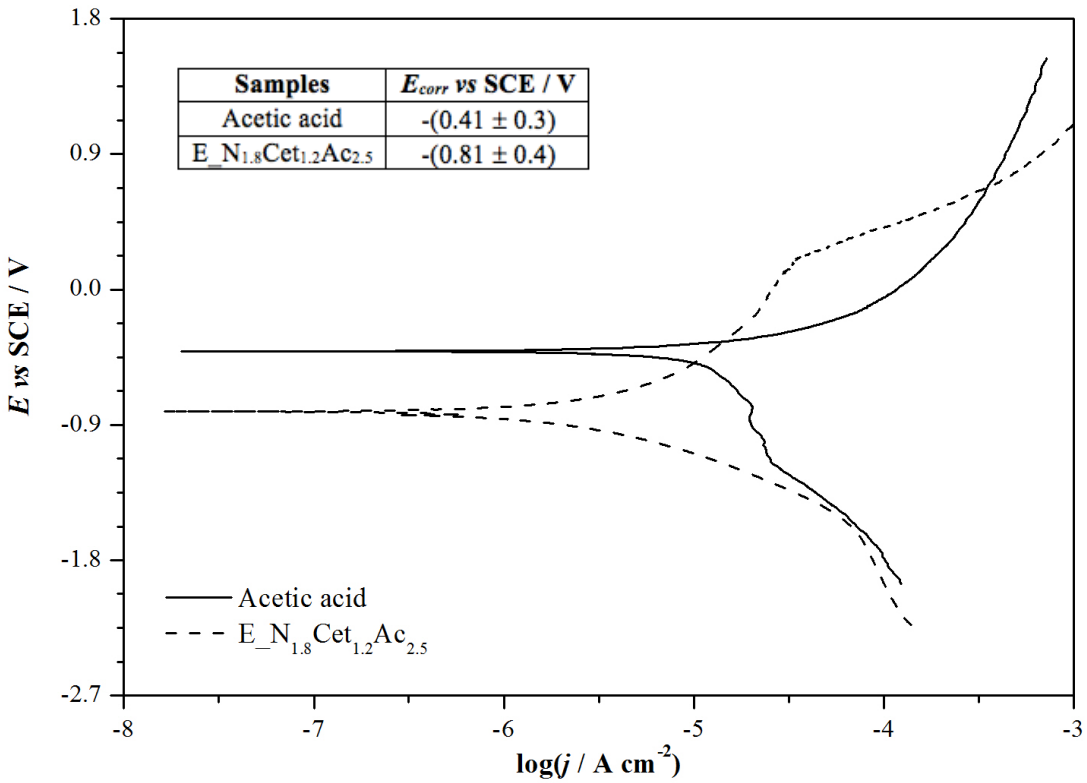
Samples
E_{corr} vs SCE / V
Acetic acid
-(0.41 ± 0.3)
E_N1.8Cet1.2Ac2.5
-(0.81 ± 0.4)
1.8
0.9
0.0
-0.9
-1.8
-2.7
E vs SCE / V
-8
-7
-6
-5
-4
-3
log(j / A cm-2)
Acetic acid
E_N1.8Cet1.2Ac2.5

FIGURE 6